

UC Davis

UC Davis Previously Published Works

Title

Characterizing Adrenergic Regulation of Glucose Transporter 4-Mediated Glucose Uptake and Metabolism in the Heart

Permalink

<https://escholarship.org/uc/item/7gg8r85g>

Journal

JACC Basic to Translational Science, 8(6)

ISSN

2452-302X

Authors

Jovanovic, Aleksandra

Xu, Bing

Zhu, Chaoqun

et al.

Publication Date

2023-06-01

DOI

10.1016/j.jacbts.2022.11.008

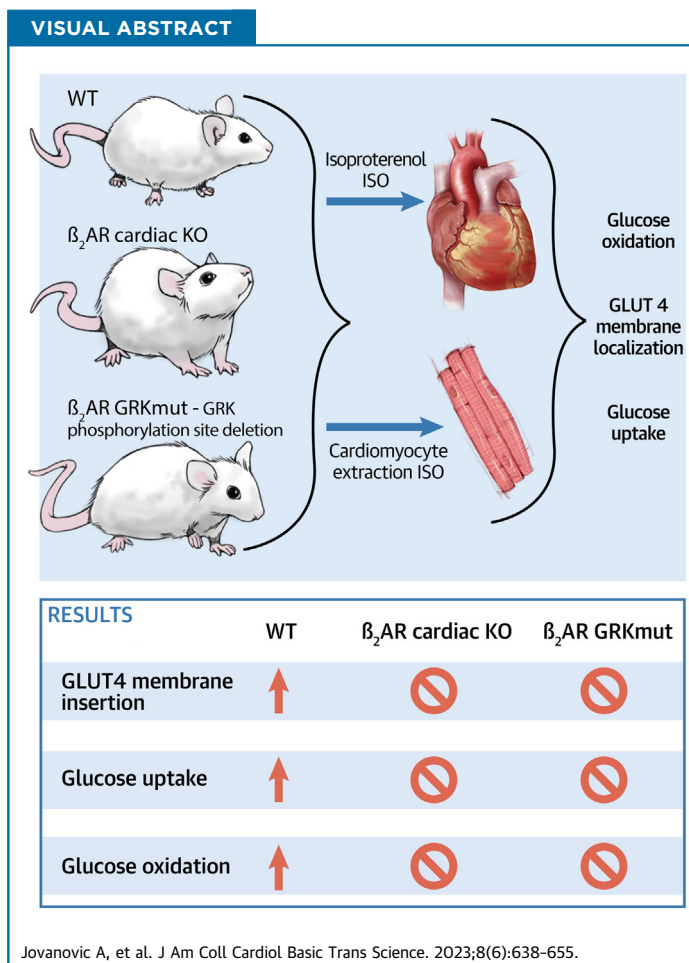
Peer reviewed

ORIGINAL RESEARCH - PRECLINICAL

Characterizing Adrenergic Regulation of Glucose Transporter 4-Mediated Glucose Uptake and Metabolism in the Heart



Aleksandra Jovanovic, PhD,^a Bing Xu, BS,^{a,b} Chaoqun Zhu, PhD,^a Di Ren, PhD,^c Hao Wang, PhD,^c Meredith Krause-Hauch, PhD,^{c,d} E. Dale Abel, PhD, MD,^e Ji Li, PhD,^{c,d} Yang K. Xiang, PhD^{a,b}



HIGHLIGHTS

- Deleting the cardiac β_2 AR abolished GLUT4 membrane insertion, glucose uptake in myocytes, and glucose oxidation in the working hearts.
- Stimulating the cardiac β_2 AR promoted a Gi-P13K-Akt cascade to drive A5160-mediated membrane insertion of GLUT4 and glucose uptake in myocytes.
- Inhibition of GRK2 and deletion of GRK phosphorylation at serine 355/356 of the β_2 AR abolished adrenergic stimulation of glucose uptake in myocytes and glucose oxidation in the working hearts.

From the ^aDepartment of Pharmacology, University of California at Davis, Davis, California, USA; ^bVeterans Affairs Northern California Health Care System, Mather, California, USA; ^cDepartment of Surgery, University of South Florida, Tampa, Florida, USA; ^dJames A. Haley Veterans Affairs Hospital, Tampa, Florida, USA; and the ^eDepartment of Medicine, David Geffen School of Medicine at University of California-Los Angeles, Los Angeles, California, USA.

SUMMARY

Whereas adrenergic stimulation promotes cardiac function that demands more fuel and energy, how this receptor controls cardiac glucose metabolism is not defined. This study shows that the cardiac β_2 adrenoceptor (β_2 AR) is required to increase glucose transporter 4 (GLUT4)-mediated glucose uptake in myocytes and glucose oxidation in working hearts via activating the cardiac β_2 AR and promotes the G inhibitory-phosphoinositide 3-kinase-protein kinase B cascade to increase phosphorylation of TBC1D4 (aka AS160), a Rab guanine triphosphatase-activating protein, which is a key enzyme to mobilize GLUT4. Furthermore, deleting G-protein receptor kinase phosphorylation sites of β_2 AR blocked adrenergic stimulation of GLUT4-mediated glucose uptake in myocytes and hearts. This study defines a molecular pathway that controls cardiac GLUT4-mediated glucose uptake and metabolism under adrenergic stimulation. (J Am Coll Cardiol Basic Trans Science 2023;8:638-655)

© 2023 The Authors. Published by Elsevier on behalf of the American College of Cardiology Foundation. This is an open access article under the CC BY-NC-ND license (<http://creativecommons.org/licenses/by-nc-nd/4.0/>).

The heart uses multiple available substrates to support the high rates of adenosine triphosphate (ATP) production and turnover that are critical for maintaining cardiac contractile function. Physiologically and in resting states, fatty acid oxidation is the primary source of ATP, contributing to ~80% of overall ATP production.^{1,2} Even though glucose is not a major source of ATP, glucose has several metabolic fates inside cardiac myocytes. Essentially, glucose is indispensable for proper cardiac function in response physiological and pathological stimuli.³ Whereas adrenergic stimulation increases cardiac function that requires increased fuel and energy, how this receptor signaling pathway controls glucose metabolism in the heart is incompletely understood.

Glucose transport across the plasma membrane is driven by a glucose gradient and occurs via facilitated diffusion. The proteins that transport glucose are members of the glucose transporter (GLUT) family. GLUT1 and GLUT4 are the main isoforms in the heart, which are insulin-independent and insulin-dependent, respectively.^{4,5} GLUT1 is dominant only during fetal and early postnatal life. Under basal conditions, it is located at the sarcolemma and has a much lower affinity for glucose than GLUT4 does.⁶ On the other hand, GLUT4 is the main isoform in differentiated cardiomyocytes, and it continuously cycles between the sarcolemma and intracellular compartments. GLUT4 has a much higher affinity for glucose and is the main GLUT isoform responsible for glucose uptake in the adult heart.^{6,7} Under basal conditions, GLUT4 is located in intracellular vesicles, whereas on

stimulation by various stimuli, including contraction, ischemia, catecholamines, and insulin, GLUT4 is translocated to the plasma membrane to facilitate glucose transport.^{8,9}

Although insulin is the primary driver of glucose uptake into skeletal muscle and adipose tissues, in cardiomyocytes, insulin signaling is not required for maintaining cardiac metabolism.¹⁰ Meanwhile, the sympathetic nervous system is another potent regulator of several metabolic pathways, including glucose homeostasis, principally via β ARs.¹¹ Several lines of evidence indicate that β_2 AR is the main isoform contributing to regulation of glucose homeostasis.¹²⁻¹⁴ Global β_2 AR deletion leads to insulin resistance and hyperglycemia in mice, and epidemiologic studies show a correlation between β_2 AR

gene variants and obesity and type 2 diabetes.¹⁴⁻¹⁶ Acute β_2 AR stimulation induces glucose uptake in skeletal myotubes in vitro and in healthy mice.^{12,13} However, the mechanisms by which β_2 AR regulates glucose metabolism in cardiac muscles under sympathetic stress is less clear.

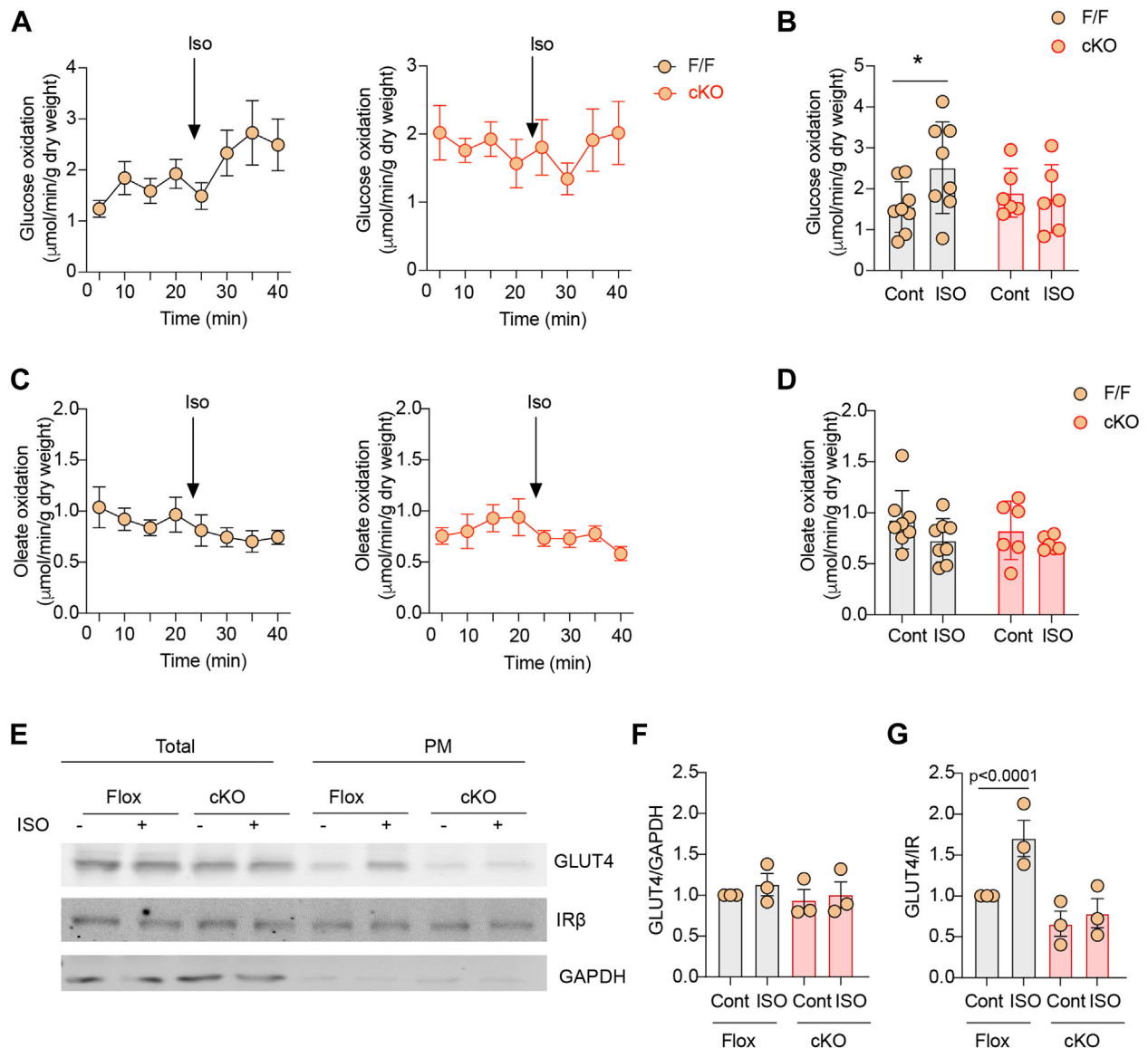
The most abundant β AR isoform in the heart is β_1 AR, which composes 75%-80% of all β ARs and is a critical regulator of cardiac contractile function. The β_2 AR contributes to the remaining 20%-25%.¹⁷ In addition to coupling to G stimulatory protein, β_2 AR may bind to pertussis toxin (PTX)-sensitive G inhibitory (G_i) protein and activate the phosphoinositide 3-kinase (PI3K)-protein kinase B (Akt) signaling pathway.^{17,18} We hypothesize that the β_2 AR is a critical

ABBREVIATIONS AND ACRONYMS

- 2-NBDG** = 2-(N-(7-nitrobenz-2-oxa-1,3-diazol-4-yl)amino)-2-deoxyglucose
- β_2 AR** = β_2 adrenoceptor
- Akt** = protein kinase B
- AMPK** = adenosine monophosphate-activated protein kinase
- AS160** = Akt substrate of 160 kDa
- ATP** = adenosine triphosphate
- AVMs** = Adult ventricular cardiomyocytes
- GAPDH** = glyceraldehyde 3-phosphate dehydrogenase
- G_i** = G inhibitory
- GLUT** = glucose transporter
- IgG** = immunoglobulin G
- ISO** = isoproterenol
- O-GlcNAc** = O-linked N-acetylglucosamine
- PAGE** = polyacrylamide gel electrophoresis
- PBS** = phosphate-buffered saline
- PI3K** = phosphoinositide 3-kinase
- PMSF** = phenylmethylsulfonyl fluoride
- PTX** = pertussis toxin
- SDS** = sodium dodecyl sulfate
- WT** = wild type

The authors attest they are in compliance with human studies committees and animal welfare regulations of the authors' institutions and Food and Drug Administration guidelines, including patient consent where appropriate. For more information, visit the [Author Center](#).

Manuscript received September 19, 2022; revised manuscript received November 18, 2022, accepted November 22, 2022.

FIGURE 1 Effects of β_2 AR Deletion on Glucose and Oleate Oxidation in Heart Under Adrenergic Stimulation

(A, B) Time course and peak response in glucose oxidation before and after stimulation with isoproterenol (ISO) (100 nmol/L). (C, D) Time course and peak response in oleate oxidation before and after stimulation with ISO (100 nmol/L). (A to D) Data represent mean \pm SEM, $n = 8$; P values were analyzed using 2-way analysis of variance with Tukey's multiple comparison test. (E) Western blot showing glucose transporter 4 (GLUT4) localization after intraperitoneal ISO injection (60 $\mu\text{g}/\text{kg}$) for 30 minutes. (F, G) The Western blots were quantified using ImageJ, and arbitrary units were defined as the ratio of intensity of GLUT4 over the intensity of insulin receptor β (IR β) for plasma membrane (PM) fractions (F) and the ratio of intensity of GLUT4 over the intensity of glyceraldehyde 3-phosphate dehydrogenase (GAPDH) for total protein level (G). Data represent mean \pm SEM, $n = 3$; * $P < 0.05$ and $P < 0.0001$ were analyzed using 2-way analysis of variance with Tukey's multiple comparison test. β_2 AR = β_2 adrenoceptor; cKO = cardiac specific β_2 AR knockout; F/F = β_2 AR flox mice.

regulator of glucose uptake in the heart by triggering the G_i -PI3K-Akt signaling pathway. Additionally, G protein-coupled receptor kinase 2 (GRK2), a kinase tightly related to β AR signaling, has also been implicated in the regulation of systemic glucose

homeostasis.¹⁹ Canonically, GRK2 phosphorylates β_2 AR and causes β arrestin-mediated β_2 AR endocytosis, eventually leading to receptor desensitization.^{20,21} Meanwhile, some studies indicate that excessive GRK2 activation leads to glucose

intolerance by mechanisms that are not completely understood.^{22,23}

In this study, we aimed to characterize the β AR subtype signaling pathways involved in glucose metabolism in the heart. Our data show that the cardiac β_2 AR is absolutely required for GLUT4-mediated glucose uptake in myocytes and isolated perfused working hearts. Activating the cardiac β_2 AR promotes Akt but not adenosine monophosphate-activated protein kinase (AMPK)-mediated phosphorylation of Akt substrate of 160 kDa (AS160) to mobilize the GLUT4 membrane insertion and glucose uptake. Furthermore, we reveal that GRK2 phosphorylation of β_2 AR is necessary for GLUT4-mediated glucose uptake. Deleting GRK phosphorylation of β_2 AR blocked adrenergic stimulation of glucose uptake in the heart. Our data define a molecular pathway that controls cardiac glucose uptake and metabolism under adrenergic stimulation.

METHODS

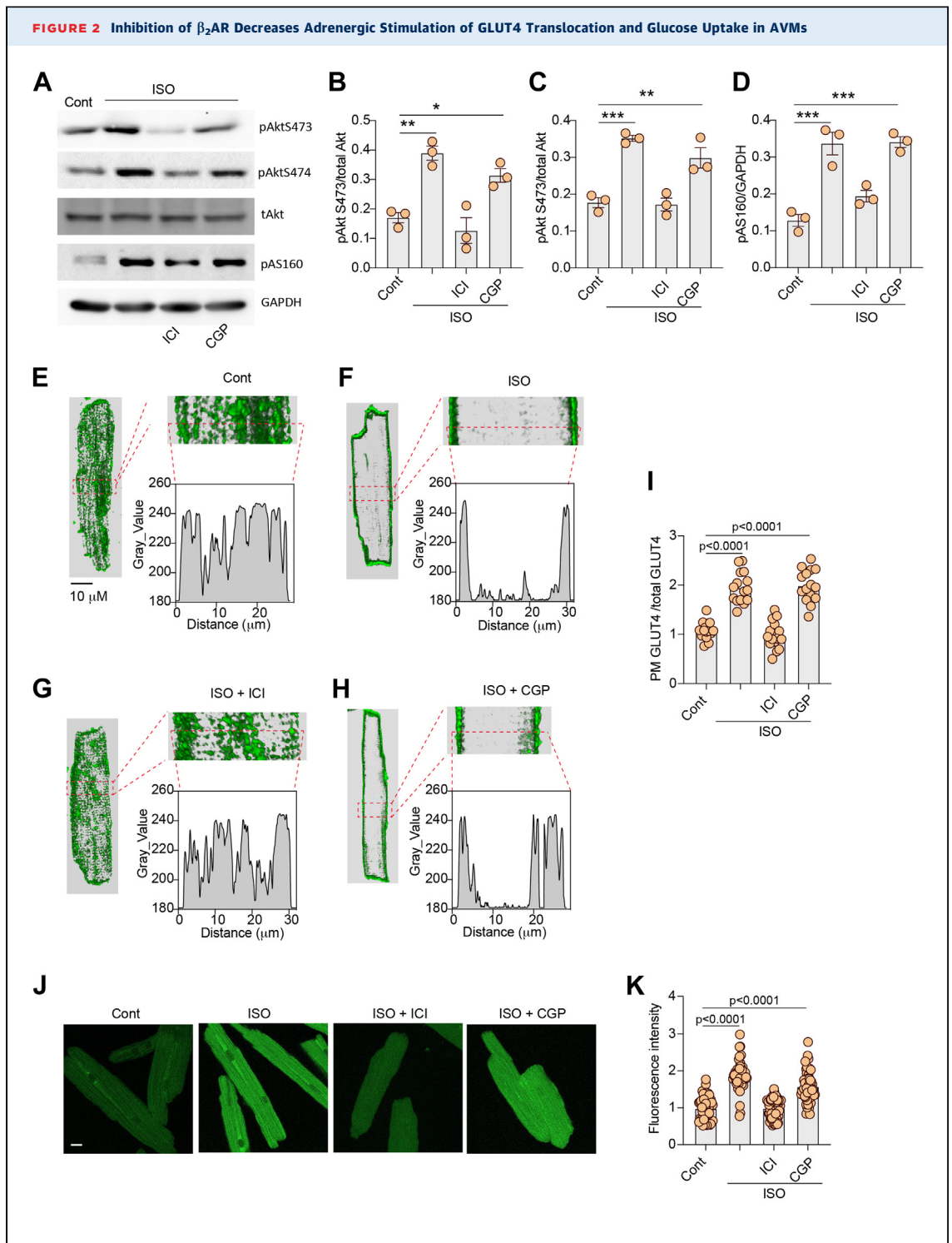
ANIMALS. β_2 AR floxed mice were a gift from Dr Gerald Karsenty (Columbia University) and were used for crossbreeding with MHC-cre (#009074; The Jackson Laboratory) to develop β_2 ARcKO. Knockin mice expressing endogenous β_2 AR lacking the GRK phosphorylation site at Ser355/356 (β_2 AR-GRK Δ) were developed by Cyagen with CRISPR technique. Mice genotypes were confirmed by polymerase chain reaction. Male β_2 ARcKO, β_2 AR-GRK Δ , and their littermate control β_2 AR flox and wild-type (WT) mice (2-3 months) were used. Male Wistar rats (2-3 months old) were also used. All the experiments were approved by the Institutional Animal Care and Use Committees (protocol 20956) of the University of California, Davis.

HEART HARVESTING AND ISOLATION OF PLASMA MEMBRANE FRACTIONS. Prior to euthanasia, mice were anesthetized under 4% isoflurane in oxygen, and body weights were recorded. Hearts were excised after thoracotomy and snap frozen in liquid nitrogen for biochemistry. Heart tissues were homogenized using glass homogenizer in osmotic lysis buffer (25 mmol/L Tris-HCl, pH 7.4; 5 mmol/L EDTA; pH 8; 1 mmol/L phenylmethylsulfonyl fluoride (PMSF); 5 mmol/L EDTA, 10 mmol/L NaF, 1 mmol/L bestatin, 1 mmol/L PMSF, 1 mmol/L benzamidimine, 2 μ g/ μ L pepstatin A, 2 mmol/L Na₃VO₄.) After homogenization, lysates were centrifuged for 5 minutes at 3,000 revolutions/min at 4 °C to remove nuclei and cell debris. The supernatant was centrifuged for 30 minutes at 23,000 revolutions/min at 4 °C. The

resulting pellet, representing plasma membrane fractions, was resuspended in radio-immunoprecipitation assay buffer (150 mmol/L NaCl; 50 mmol/L Tris-HCl, pH 8; 1% Nonidet P-40 [Shell Chemical]; 0.5% sodium deoxycholate, 0.1% sodium dodecyl sulfate [SDS]) for Western blotting. Protein concentration was measured using BCA Kit (23225, Thermo Fisher Scientific). Equal amounts of protein (30 μ g) were loaded in each well and resolved on 8% SDS-polyacrylamide gel electrophoresis (PAGE) gel. After transfer, membranes were stained with anti-GLUT4 antibody (1:1000, ab654; Abcam), anti-insulin receptor β antibody (C-19, rabbit polyclonal immunoglobulin G [IgG], SC-711; Santa Cruz Biotechnology), or anti-glyceraldehyde 3-phosphate dehydrogenase (GAPDH) (1:10000, MAB374; Millipore) antibodies. Primary antibodies were detected either with IRDye 800 CW Goat anti-Rabbit IgG secondary antibody (1:10000, #926-32211; Licor) or IRDye 800CW Goat anti-Mouse IgG secondary antibody (1:10000, #926-32210; Licor) using ChemiDoc Imaging System (Bio-Rad). The optical density of the band was analyzed using ImageJ software (National Institutes of Health)

ECHOCARDIOGRAPHY. Mice were anaesthetized with isoflurane (2%) in oxygen and placed on a warm pad with electrocardiogram monitoring. The heart rates were kept consistent between 450 and 500 beats/min at baseline to avoid variation. Left ventricular systolic and diastolic functions were assessed using M-mode, tissue Doppler, and Doppler echocardiography using a Vevo 2100 Imaging System with a 22-25 MHz MS550D linear probe (Visual Sonic). After baseline measurement, mice were injected with isoproterenol (ISO) (100 ng/g) intraperitoneally. Cardiac functions were assessed with echocardiography.

CARDIOMYOCYTE ISOLATION, CELL CULTURE, AND ADENOVIRUS INFECTION. Adult ventricular cardiomyocytes (AVMs) from mice and rats were isolated as previously described.^{24,25} Briefly, mice or rats were anesthetized using isoflurane, and hearts were excised and mounted on the Langendorff perfusion system. After that, hearts were perfused with a collagenase and protease solution (0.5 mg/mL collagenase and 0.1 mg/mL protease per mouse; 1 mg/mL collagenase and 0.2 mg/mL protease per rat). Freshly isolated AVMs were plated on mouse laminin (Life Technologies)-coated dishes in minimum essential medium (M1018; Sigma-Aldrich), supplemented with 1% penicillin-streptomycin-glutamine, 4 mmol/L NaHCO₃, 0.2% bovine serum albumin, 10 mmol/L HEPES (N-2-hydroxyethylpiperazine-N-2-ethane sulfonic acid), and 6.25 μ mol/L blebbistatin.



Continued on the next page

Recombinant adenoviruses were generated with pAdeasy system (Qbiogene) as previously described.²⁶ AVMs were infected with adenovirus at multiplicity of infection of 100 for 24 hours.

IMMUNOFLUORESCENCE AND CONFOCAL MICROSCOPY. Isolated AVMs were plated on laminin-coated glass coverslips and cultured for 2 hours. After that, the cells were either treated with the appropriate

inhibitors, followed by ISO stimulation, or infected with WT β_2 AR or GRK knockin β_2 AR for 24 hours followed by ISO stimulation. The cells were fixed in 4% paraformaldehyde for 15 minutes at room temperature and washed with phosphate-buffered saline (PBS) 3 \times for 15 minutes. Cell permeabilization was done using 0.2% Triton-X100 for 15 minutes, followed by blocking in 5% goat serum in PBS for 1 hour. The cells were stained with anti-GLUT4 antibody (1:250, ab654; Abcam) overnight at 4 °C. After washing 3 \times for 15 minutes, cells were incubated in a secondary antibody, Goat-anti-Rabbit Alexa Fluor 488 (1:1000, A-11008; Thermo Fisher Scientific), for 1 hour at room temperature. The cells were washed 3 \times for 15 minutes in PBS before mounting with Mountant and PermaFluor (Thermo Fisher Scientific). Super-resolution images were obtained using the LIGHTNING mode in TCS SP8 Falcon confocal microscope (Leica), 63 \times /1.3 oil immersion lens. Randomized images of 15-30 different cells from 3-5 independent experiments were used to analyze GLUT4 translocation using the ImageJ software.

GLUT4 TRANSLOCATION ANALYSIS. GLUT4 translocation analysis was performed using the ImageJ software. Briefly, for each cardiomyocyte, a (region of interest band was designed across the cell, and the fluorescence intensity was measured. The sum of fluorescence intensity in the membrane regions of the cell (2-3 μ m near the edge of the cell) was normalized to total fluorescence intensity.

GLUCOSE UPTAKE MEASUREMENT. For glucose uptake measurements, cardiomyocytes were plated on laminin-coated glass coverslips and cultured for 2 hours. After that, the medium was replaced by PBS, and the cells were treated with the appropriate inhibitors, followed by ISO stimulation. After 10 minutes, the cells were loaded with 100 μ mol/L

2-(N-(7-nitrobenz-2-oxa-1,3-diazol-4-yl)amino)-2-deoxyglucose (2-NBDG) (Life Technologies) for 20 minutes in the dark. After 1 wash in PBS, cells were fixed with 4% paraformaldehyde and mounted with Mountant and PermaFluor (Thermo Fisher Scientific). Super-resolution images were obtained using the LIGHTNING mode in TCS SP8 Falcon confocal microscope (Leica), 63 \times /1.3 oil immersion lens. Randomized images of 30-50 different cells from 3-5 independent experiments were used to analyze GLUT4 translocation in ImageJ software.

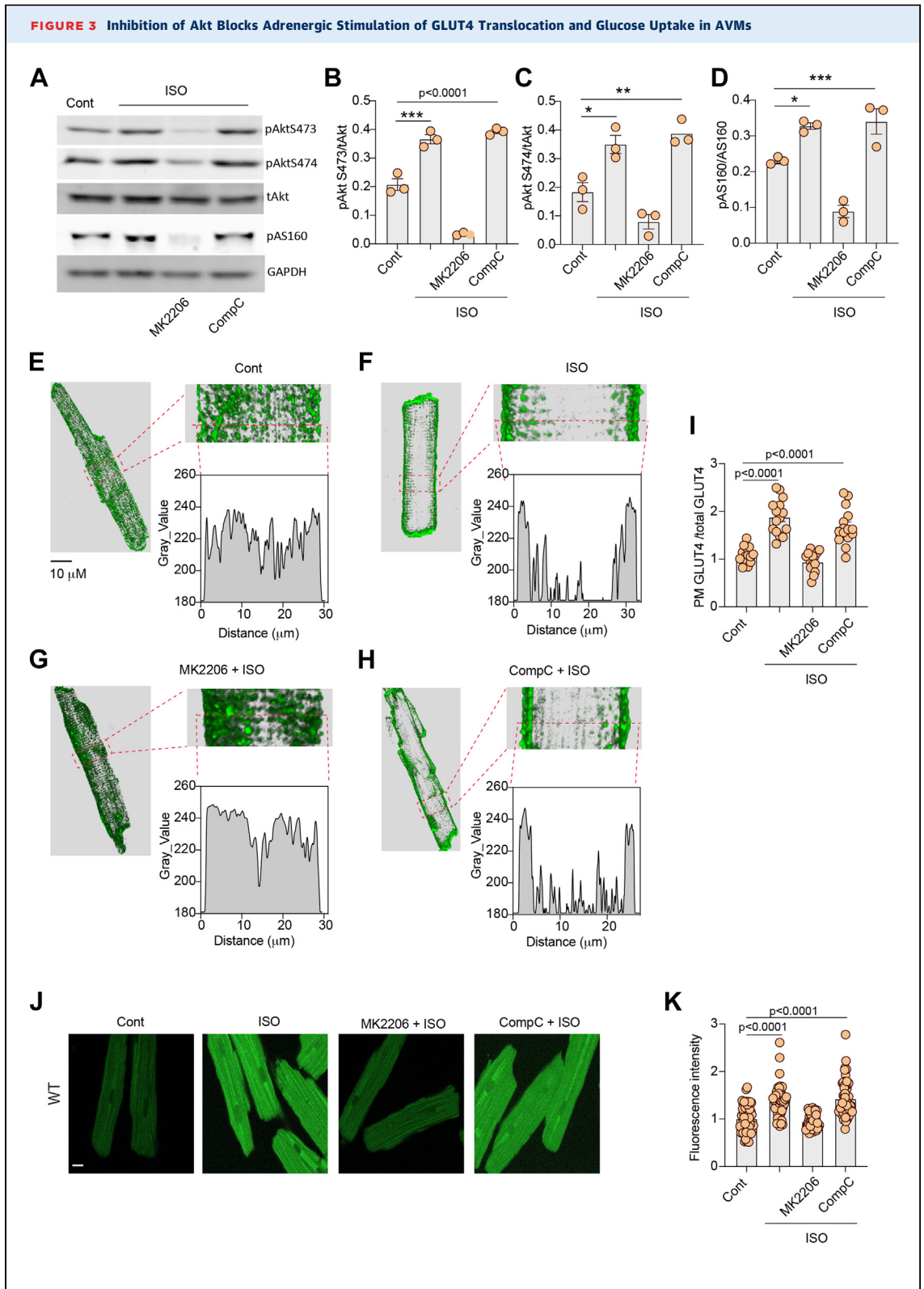
MYOCARDIAL SUBSTRATE USE AND CONTRACTILE FUNCTION IN ISOLATED WORKING MOUSE HEARTS.

Myocardial substrate use and contractile function were measured as described previously.²⁷ Briefly, mice were anesthetized using isoflurane. Hearts were excised and mounted on a working heart system. Hearts were first retrogradely perfused via aorta with Standard Krebs-Henseleit buffer supplemented with 8 mmol/L glucose, 0.4 mmol/L oleate conjugated to 3% bovine serum albumin (fraction V, fatty acid-free; dialyzed), 10 μ U/mL insulin (basal/fasting concentration), as well as radiolabeled tracers: 1) [U-14C]-glucose (0.12 mCi/L from MP Biomedicals; glucose oxidation); and 2) [9, 10-3H]-oleate (0.067 mCi/L from Sigma-Aldrich; β -oxidation). The pulmonary vein was then cannulated while the heart switched to the working mode with buffer pumped via the pulmonary vein to the left atrium and ejected via the aorta. Then 2-3 mL of buffer sample from the coronary sinus was collected every 5 minutes for 20 minutes before and 20 minutes after ISO stimulation and used to measure ¹⁴CO₂ (representing glucose oxidation) and ³H₂O (representing oleate oxidation).

WESTERN BLOTTING. Left ventricular tissue and AVMs were used for Western blotting. Heart tissues were lysed using glass homogenizer in radio-immunoprecipitation assay buffer (150 mmol/L NaCl;

FIGURE 2 Continued

(A) Western blots showing phosphorylation of protein kinase B (Akt) at Ser473 and Ser474 and phosphorylation (p) of Akt substrate of 160 kDa (AS160) at Thr172 in rat adult ventricular cardiomyocytes (AVMs) after stimulation with ISO (100 nmol/L, 10 minutes) or after pretreatment with β_2 AR antagonist ICI118551 (ICI) (100 nmol/L, 5 minutes) or β_1 AR antagonist CGP20712a (CGP) (300 nmol/L, 5 minutes) followed by stimulation with ISO. The Western blots were quantified using ImageJ, and arbitrary units were defined as the ratio of intensity of pAkt over the intensity of total (t) Akt (**B, C**) or as the ratio of intensity of pAS160 over the intensity GAPDH (**D**). (**B to D**) Data represent mean \pm SEM, n = 3; *P < 0.05, **P < 0.01, and ***P < 0.001 were analyzed using 1-way analysis of variance with Tukey's multiple comparison test. (**E-H**) Representative confocal images of GLUT4 staining and quantification of GLUT4 translocation (**I**) after stimulation with ISO (100 nmol/L, 30 minutes) or after pretreatment with β_2 AR antagonist ICI (100 nmol/L, 5 minutes) or β_1 AR antagonist CGP (300 nmol/L, 5 minutes) followed by stimulation with ISO. (**J**) Representative confocal images of 2-(N-(7-nitrobenz-2-oxa-1,3-diazol-4-yl)amino)-2-deoxyglucose (2-NBDG) uptake and 2-NBDG uptake quantification (**K**) after stimulation with ISO (100 nmol/L, 30 minutes) or after pretreatment with β_2 AR antagonist ICI (100 nmol/L, 5 minutes) or β_1 AR antagonist CGP (300 nmol/L, 5 minutes) followed by stimulation with ISO. (**I, K**) Data represent mean \pm SEM of myocytes from 3 mice; P < 0.0001 were obtained using 1-way analysis of variance with Tukey's multiple comparison test. Cont = control; other abbreviations as in Figure 1.



Continued on the next page

50 mmol/L Tris-HCl, pH 8; 1% Nonidet P-40; 0.5% sodium deoxycholate, 0.1% SDS) supplemented with protease and phosphatase inhibitors (5 mmol/L EDTA, 10 mmol/L NaF, 1 mmol/L bestatin, 1 mmol/L PMSF, 1 mmol/L benzamidimine, 2 µg/µL pepstatin A, 2 mmol/L Na₃VO₄), and then centrifugated at 13,000 revolutions/min for 10 minutes. Freshly isolated AVMs were plated in laminin-coated 6-well plates and cultured for 2 hours. After that, the cells were treated with appropriate inhibitors followed by stimulation with ISO for 10 minutes. The cells were lysed in SDS-PAGE loading buffer (10% SDS, 5% β-mercaptoethanol, 50% glycerol, 500 mmol/L Tris-HCl, 0.05% bromophenol blue dye). Equal volumes (15 µL for AVMs lysates) or equal amount of protein (30 µg for left ventricular tissue lysates) were loaded and resolved on an SDS-PAGE gel, followed by detection with: anti-phospho-AS160 (TBC1D1 pThr 642) (1:1000, #4288; Cell Signaling Technology), anti-phospho-Akt Ser473 (1:2000, #4051; Cell Signaling Technology), anti-phospho-Akt2 Ser474 (1:2000, #5899; Cell Signaling Technology), anti-phospho-Akt Thr308 (1:1000, #2965; Cell Signaling Technology), anti-total-Akt (1:1000, #2920; Cell Signaling Technology), anti-GAPDH (1:10 000, MAB374; Millipore), anti-phospho-mTOR Ser2481 (1:1000; Cell Signaling Technology), anti-phospho-PDPK1 Ser241 (1:1000, #3438; Cell Signaling Technology), anti-total-PDPK1 (1:1000, #3062; Cell Signaling Technology), anti-phospho-AMPK Thr172 (1:1000, #50081S; Cell Signaling Technology), anti-GRK2 (1:1000, C9; Santa Cruz Biotechnology), anti-GRK5 (1:1000, h-64; Santa Cruz Biotechnology), anti-βarrestin2 (1:1000, SC13140; Santa Cruz Biotechnology), anti-Gαi (1:1000, sc13533; Santa Cruz Biotechnology), anti-GLUT4 (1:1000, ab654; Abcam). All primary antibodies were detected either with IRDye 800 CW Goat anti-Rabbit IgG secondary antibody (1:10000, #926-32211; Licor) or IRDye 800CW Goat anti-Mouse IgG secondary antibody

(1:10000, #926-32210; Licor) using ChemiDoc Imaging System (Bio-Rad). The optical density of the band was analyzed using ImageJ software. The arbitrary units were defined as the ratio of optical density of protein of interest over the reference protein or the density of phosphorylated protein over the total protein.

DATA ANALYSIS. Data are represented as mean ± SEM. Animals were grouped in a randomized fashion during the experiments. Each animal was assigned a unique identification number. Subsequently, the numbers were drawn “out of a hat” and randomly assigned to different groups. Blinded analysis was performed such that different persons carried out the experiments and subsequent analysis. Representative images and figures reflect the average level of each experiment. The data normality was tested by D’Agostino-Pearson normality test, using Prism software (version 9.0; GraphPad). Comparisons between 2 groups were determined using paired or unpaired 2-tailed Student’s *t*-test, whereas comparisons among >2 groups were done using 1- or 2-way analysis of variance, followed by Tukey’s post hoc test for multiple pairwise comparisons. All bar graphs represent the mean ± SEM. A value of *P* < 0.05 was considered to be statistically significant.

AVAILABILITY OF DATA AND MATERIALS. The data sets supporting the conclusions of this article are included within the article and its [Supplemental Appendix](#).

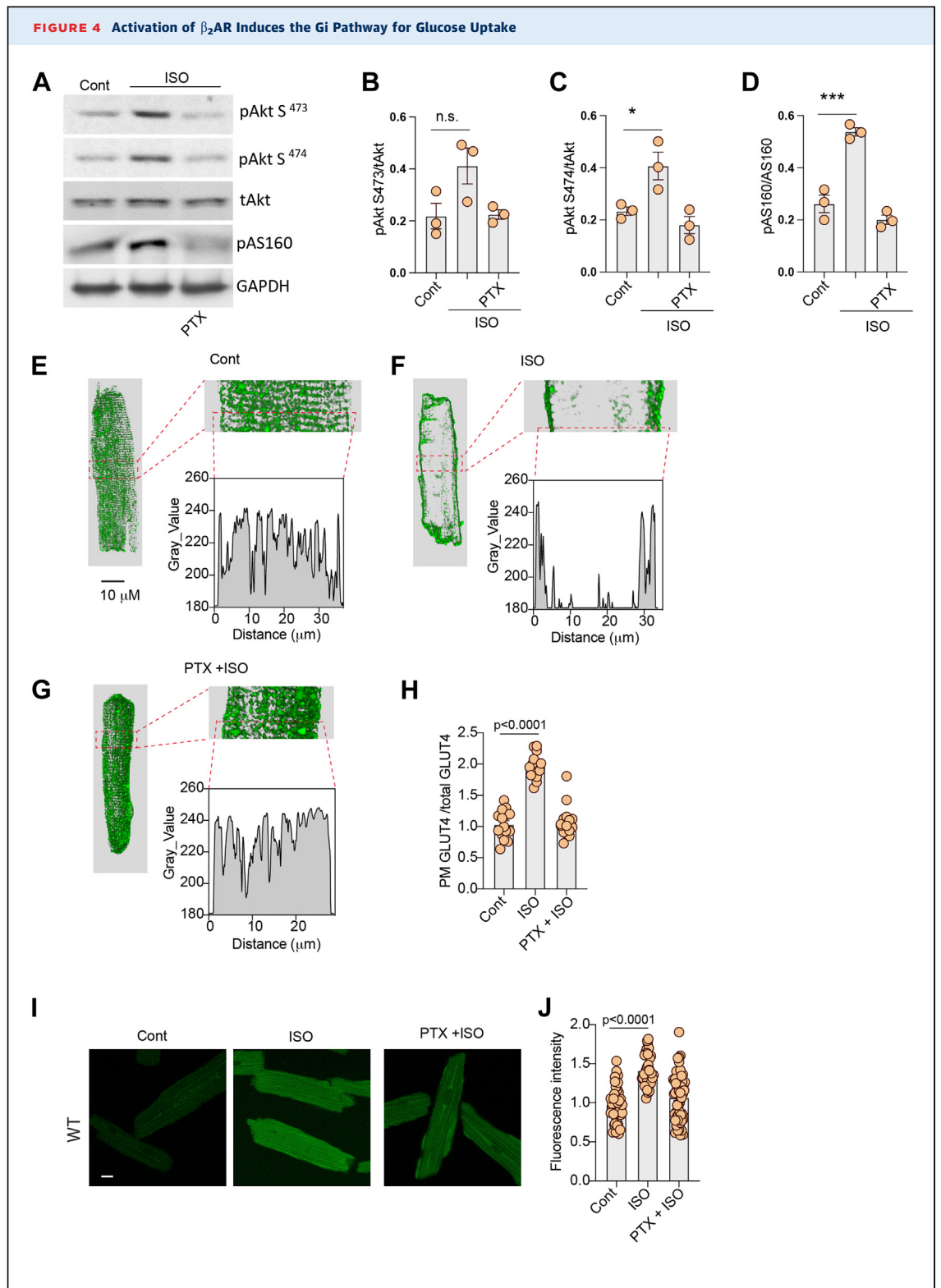
RESULTS

Mice with cardiomyocyte-specific deletion of β₂AR (β₂AR-CKO) were grossly normal with similar cardiac function at the baseline and after adrenergic stimulation when compared to flox control mice ([Supplemental Table 1](#)). β₂AR-CKO and flox mice were then used to examine the role of β₂AR in glucose uptake and oxidation in hearts. Hearts from β₂AR-CKO

FIGURE 3 Continued

(A) Western blots showing pAkt at Ser473 and Ser474 and pAS160 at Thr172 in rat AVMs after stimulation with ISO (100 nmol/L, 10 minutes) or after pretreatment with Akt inhibitor MK2206 (10 µmol/L, 30 minutes) or adenosine monophosphate-activated protein kinase inhibitor CompoundC (CompC) (10 µmol/L, 30 minutes) followed by stimulation with ISO. **(B to D)** The Western blots were quantified using ImageJ, and arbitrary units were defined as the ratio of intensity of pAkt over the intensity of tAkt **(B, C)** or as the ratio of intensity of pAS160 over the intensity GAPDH **(D)**. Data represent mean ± SEM, n = 3; **P* < 0.05, ***P* < 0.01, ****P* < 0.001, and *P* < 0.0001 were analyzed using one-way analysis of variance with Tukey’s multiple comparison test. **(E to H)** Representative confocal images of GLUT4 staining and quantification of GLUT4 translocation **(I)** after stimulation with ISO (100 nmol/L, 30 minutes) or after pretreatment with MK2206 (10 µmol/L, 30 minutes) or CompC (10 µmol/L, 30 minutes) followed by stimulation with ISO. **(J)** Representative confocal images of 2-NBDG uptake and 2-NBDG uptake quantification **(K)** after stimulation with ISO (100 nmol/L, 30 minutes) or after pretreatment with MK2206 (10 µmol/L, 30 minutes) or CompC (10 µmol/L, 30 minutes) followed by stimulation with ISO. **(I, K)** Data represent mean ± SEM of myocytes from 3 mice; *P* < 0.0001 were analyzed using 1-way analysis of variance with Tukey’s multiple comparison test. WT = wild type; other abbreviations as in

[Figures 1 and 2](#).



Continued on the next page

and flox controls were subjected to working heart perfusion with electropacing to establish a working heart model. In the working hearts, deletion of β_2 AR in myocytes minimally affects cardiac function at the baseline and after adrenergic stimulation with β AR agonist ISO (100 nmol/L) (Supplemental Table 2). Glucose oxidation was measured at the baseline and after infusion of ISO. Stimulation with ISO significantly increased glucose oxidation in flox hearts (Figures 1A and 1B). However, deleting the β_2 AR, abolished the ISO-induced increases in glucose oxidation (Figures 1A and 1B). Meanwhile, stimulation with ISO slightly reduced oleate oxidation in working hearts from both β_2 AR-CKO and flox mice (Figures 1C and 1D). Consistent with increased glucose use, ISO injection significantly enhanced membrane insertion of GLUT4 in flox hearts in vivo, which was blocked in β_2 AR-CKO hearts (Figures 1E and 1F). We also examined expression levels of regulatory proteins that are relevant to GLUT4 translocation and glucose uptake. Activation of β_2 AR is known to stimulate G_i -dependent activation of the PI3K-Akt signaling cascade. Here, deleting the β_2 AR did not affect the expression of G_i , p85 of PI3K, and GLUT4 expression, nor did it affect the expression of other adrenergic signaling proteins such as GRK2, GRK5, and β arrestin2 expression in the hearts (Supplemental Figure 1). Additionally, deleting the β_2 AR minimally affected the baseline phosphorylation of mTOR, PDPK1, Akt, AMPK, and AS160 (Supplemental Figure 2).

We then assessed the role of direct β_2 AR activation in the regulation of GLUT4 membrane insertion and glucose uptake in AVMs isolated from rat hearts. AVMs were pretreated with either β_2 AR selective blocker ICI118551 or β_1 AR selective blocker CGP20712a before stimulation with ISO to selectively activate β_1 AR and β_2 AR, respectively. Stimulation with ISO induced an increase in Akt phosphorylation at S473 and S474 and AS160 phosphorylation at Thr172 in AVMs (Figures 2A to 2D). Pretreatment with ICI118551, but not CGP20712a, blocked ISO-induced

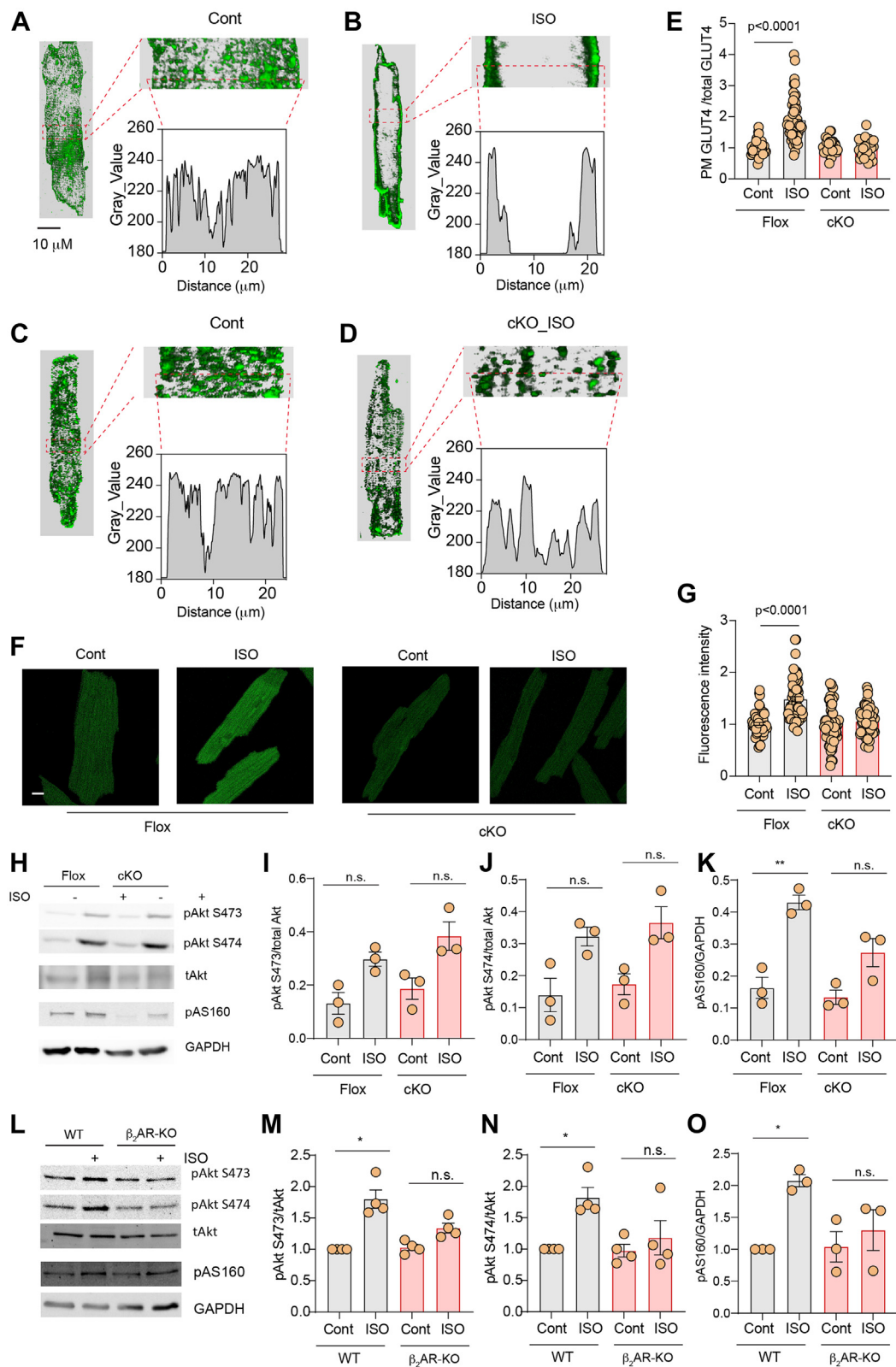
phosphorylation of Akt and AS160 (Figures 2A to 2D). Although stimulation with ISO induced translocation of endogenous GLUT4 from the intracellular compartment to the plasma membrane in AVMs, inhibition of β_2 AR with ICI118551 completely blocked the GLUT4 membrane insertion (Figures 2E to 2I). Inhibition of β_1 AR with CGP20712a did not affect the ISO-induced GLUT4 membrane insertion (Figures 2E to 2I). In agreement, inhibiting β_2 AR with ICI118551 completely blocked glucose uptake into AVMs, whereas inhibiting β_1 AR with CGP20712a did not (Figures 2J and 2K).

Both AMPK and Akt are implicated in GLUT4 translocation and membrane insertion leading to increased glucose uptake in relevant cell types. We examined which kinases are involved in adrenergic stimulation of glucose uptake in AVMs. Inhibition of Akt with MK2206 completely blocked ISO-induced phosphorylation of Akt and AS160, whereas inhibition of AMPK with CompoundC did not block ISO-induced phosphorylation of Akt and AS160 in AVMs (Figures 3A to 3D). Inhibiting Akt with MK2206 blocked the GLUT4 membrane insertion induced by ISO, whereas inhibiting AMPK with CompoundC did not (Figures 3E to 3I). In agreement, inhibiting Akt with MK2206 blocked glucose uptake into AVMs, whereas inhibiting AMPK with CompoundC did not affect the ISO-induced glucose uptake (Figures 3J and 3K). We then assessed whether G_i coupling is necessary for β_2 AR stimulation of Akt signal for GLUT4 translocation and glucose uptake. Pretreatment with G_i inhibitor PTX abolished ISO-induced increases in Akt and AS160 phosphorylation in AVMs (Figures 4A to 4D). Pretreatment with PTX blocked the GLUT4 membrane insertion and glucose uptake into AVMs induced by ISO (Figures 4E to 4L). Together these data suggest that stimulation of β_2 AR leads to G_i -Akt-mediated GLUT4 translocation and glucose uptake in AVMs.

We further independently assessed the role of β_2 AR in the regulation of GLUT4 membrane insertion

FIGURE 4 Continued

(A) Western blots showing pAkt at Ser473 and Ser474 and pAS160 at Thr172 in rat AVMs after stimulation with ISO (100 nmol/L, 10 minutes) or after pretreatment with G_i inhibitor, pertussis toxin (PTX) (500 ng/mL, 3 hours) followed by stimulation with ISO. The Western blots were quantified using ImageJ, and arbitrary units were defined as the ratio of intensity of pAkt over the intensity of tAkt (B, C) or as the ratio of intensity of pAS160 over the intensity of GAPDH (D). (B to D) Data represent mean \pm SEM of myocytes from 3 mice; * $P < 0.05$ and *** $P < 0.001$ were analyzed using 1-way analysis of variance with Tukey's multiple comparison test. (E to G) Representative confocal images of GLUT4 staining and (H) quantification of GLUT4 translocation in rat AVMs after stimulation with ISO (100 nmol/L, 10 minutes) or after pretreatment with PTX (500 ng/mL, 3 hours) followed by stimulation with ISO. (I) Representative confocal images of 2-NBDG uptake and (J) 2-NBDG uptake quantification in rat AVMs after stimulation with ISO (100 nmol/L, 10 minutes) or after pretreatment with PTX (500 ng/mL, 3 hours) followed by stimulation with ISO. (H, J) Data represent mean \pm SEM, $n = 3$; **** $P < 0.0001$ were analyzed using 1-way analysis of variance with Tukey's multiple comparison test. NS = not significant; other abbreviations as in Figures 1 to 3.

FIGURE 5 β_2 AR Deletion Decreases Adrenergic Stimulation of GLUT4 Translocation and Glucose Uptake in AVMs

and glucose uptake in AVMs isolated from β_2 AR-CKO hearts. Whereas stimulation with ISO significantly relocated GLUT4 from the intracellular compartment to the PM in flox AVMs, the GLUT4 translocation was inhibited in β_2 AR-CKO AVMs (Figures 5A to 5E). Deleting β_2 AR also blocked glucose uptake into β_2 AR-CKO AVMs (Figures 5F and 5G). Interestingly, stimulation with ISO increased Akt phosphorylation at S473 and S474 in β_2 AR-CKO hearts and in isolated β_2 AR-CKO AVMs (Supplemental Figures 3A and 3B). However, deletion of β_2 AR significantly attenuated ISO-induced increases in phosphorylation of AS160 in β_2 AR-CKO hearts relative to the flox control hearts (Figures 5H and 5I). Moreover, global deletion of β_2 AR completely abolished ISO-induced increases in phosphorylation of Akt and AS160 in hearts (Figures 5J and 5K). Together, these data indicate that cardiac β_2 AR is necessary to stimulate Akt and AS160 for GLUT4 translocation and glucose uptake in hearts.

We recently identified 2 subpopulations of β_2 AR that undergo phosphorylation selectively by GRK and protein kinase A, respectively. Previous studies indicate that GRK2 affects glucose uptake.^{28,29} We postulated that a subpopulation of GRK-phosphorylated β_2 AR may be essential for the activation of Akt and AS160 in glucose uptake. First, we applied a pharmacologic inhibitor of GRK2 in AVMs. Inhibition of GRK2 with paroxetine blocked ISO-induced translocation of GLUT4 and glucose uptake in rat AVMs (Figures 6A to 6G). Paroxetine is also a serotonin inhibitor. Fluoxetine is another serotonin inhibitor without the inhibitory effect of GRK2. As a control, fluoxetine did not affect the ISO-induced membrane insertion of GLUT4 and glucose uptake in AVMs (Figures 6A to 6G). We also attempted to reintroduce WT and mutant β_2 AR lacking the GRK phosphorylation sites at Ser355/356 (GRKmut). Introducing WT- β_2 AR in β_2 AR-CKO AVMs restored ISO-induced GLUT4 translocation and glucose uptake, whereas introducing GRKmut- β_2 AR failed to recover the ISO-induced effects in β_2 AR-CKO AVMs (Figures 6H to 6N, Supplemental Figure 4A). These

data indicate that inhibition of GRK2 or deleting GRK phosphorylation of β_2 AR blocks adrenergic stimulation of GLUT4 translocation and glucose uptake in AVMs.

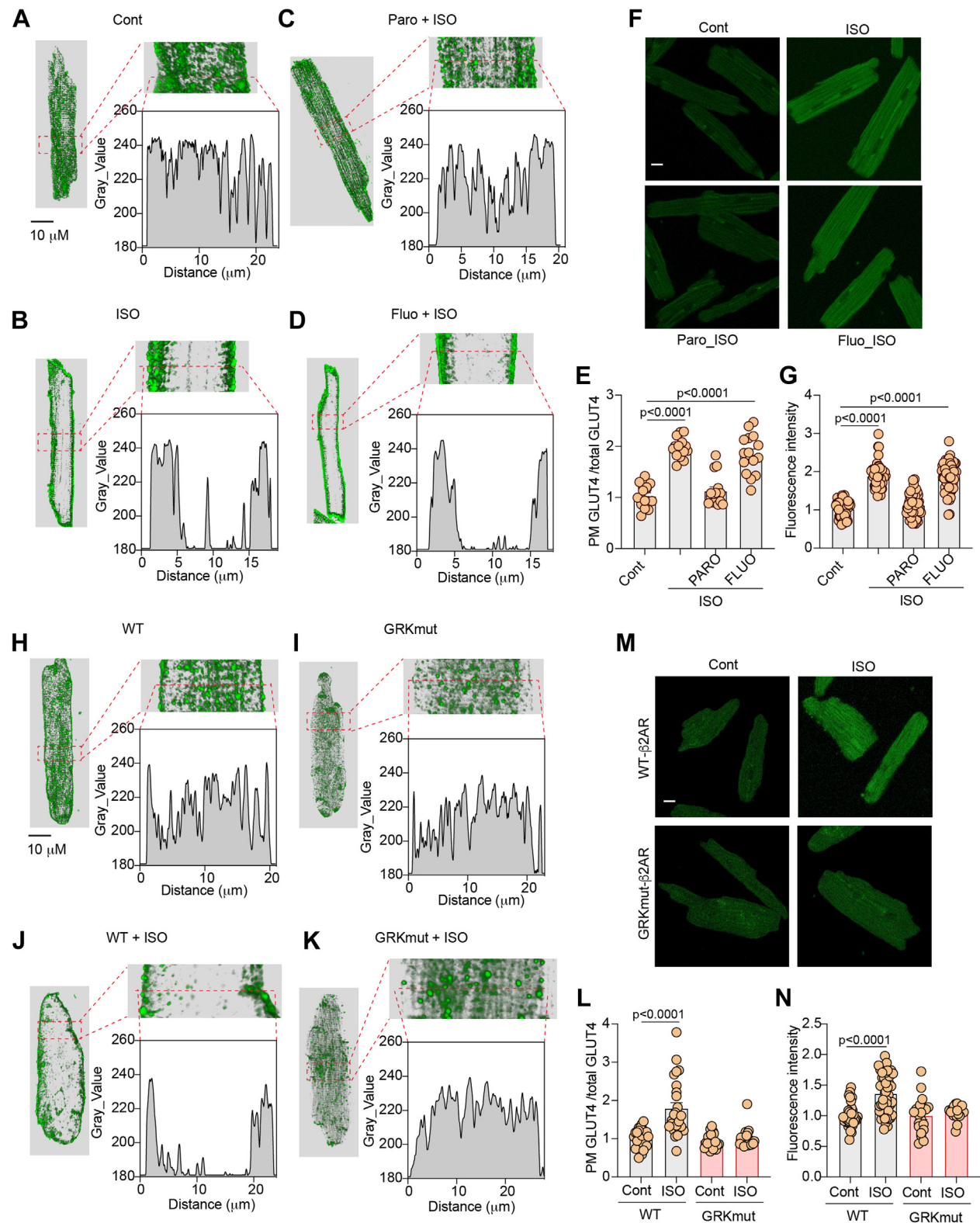
We further examined the role of the subpopulation of GRK-phosphorylated β_2 AR in glucose uptake in vivo. We have developed CRISPR knockin mice expressing endogenous β_2 AR lacking the GRK phosphorylation site at Ser355/356 (GRKD), which were replaced with alanine. GRKD mice were grossly normal and displayed similar cardiac function at the baseline and after adrenergic stimulation when compared to WT control mice (Supplemental Table 3). GRKD did not affect the cardiac expression of GLUT4, GRK2, β arrestin, and the p85 subunit of PI3K (Supplemental Figures 5A and 5B). GRKD hearts displayed similar phosphorylation of Akt and elevated phosphorylation of AS160 (Supplemental Figures 5C and 5D). In comparison to WT AVMs, stimulation of GRKD AVMs failed to translocate GLUT4 to the PM and increase glucose uptake (Figures 7A to 7G). Both WT and GRKD hearts display similar cardiac functions in isolated working hearts at the baseline and after adrenergic stimulation (Supplemental Table 4). Whereas stimulation with ISO enhanced glucose oxidation in WT hearts, it did not increase glucose oxidation in GRK knockin hearts (Figures 7H and 7I). Meanwhile, GRKD hearts displayed an elevation of oleate oxidation at the baseline, but ISO stimulation did not alter oleate oxidation in WT and GRKD hearts (Figures 7J and 7K). These data confirm that the subpopulation of GRK phosphorylated β_2 AR is necessary for stimulation of glucose uptake and use in hearts.

DISCUSSION

Glucose is a critical fuel for maintaining cardiac function in response (patho)physiological stress. Adrenergic stimulation promotes cardiac function, which requires increased substrate metabolism and energy consumption, but how this receptor signaling controls glucose metabolism in hearts is incompletely

FIGURE 5 Continued

(A to D) Representative confocal images of GLUT4 staining and quantification of GLUT4 translocation (E) in AVMs isolated from β_2 AR flox or β_2 AR CKO mice after stimulation with ISO (100 nmol/L, 30 minutes). (F) Representative confocal images of 2-NBDG uptake and 2-NBDG uptake quantification (G) in AVMs isolated from β_2 AR flox or β_2 AR CKO mice after stimulation with ISO (100 nmol/L, 30 minutes). (E, G) Data represent mean \pm SEM of myocytes from 3 mice; $P < 0.0001$ were analyzed using two-way analysis of variance with Tukey's multiple comparison test. (H, L) Western blots showing pAkt at Ser473 and Ser474 and pAS160 at Thr172 after intraperitoneal ISO injection (60 μ g/kg) 10 minutes prior to organ harvest in β_2 AR flox, β_2 AR-CKO, WT, and β_2 AR whole body knockout (KO), respectively. (I to K, M to O) Data represent mean \pm SEM, $n = 3-4$; * $P < 0.05$ and ** $P < 0.01$ were obtained using two-way analysis of variance with Tukey's multiple comparison test. Abbreviations as in Figures 1 to 4.

FIGURE 6 GRK2 Phosphorylation of β_2 AR Is Necessary for Adrenergic Stimulation of GLUT4 Translocation and Glucose Uptake in AVMs

understood. Our data reveal that the cardiac β_2 AR is absolutely required to stimulate GLUT4-mediated glucose uptake in myocytes and isolated whole working hearts. Activating the cardiac β_2 AR promotes Akt-mediated phosphorylation of AS160 to mobilize GLUT4 membrane insertion and glucose uptake. Furthermore, our data reveal that the phosphorylation of β_2 AR by GRK2 is necessary for GLUT4-mediated glucose uptake. Deleting the GRK phosphorylation of β_2 AR completely prevented adrenergic stimulation of glucose uptake in the heart. Our data define the molecular pathway that controls cardiac glucose uptake and use under adrenergic stimulation.

Under basal conditions, GLUT4 is located in intracellular compartments, whereas on stimulation by various stimuli, including contraction, ischemia, catecholamines, and insulin, GLUT4 is translocated to the plasma membrane to facilitate glucose transport.³⁰ Our data show that deletion of the cardiac β_2 AR abolished GLUT4 membrane insertion in the hearts and abrogated the increases in glucose metabolism in working hearts after stimulation of ISO. These observations suggest that the cardiac β_2 AR is necessary for increasing cardiac glucose metabolism, even though previous studies show that contraction can stimulate glucose uptake.³¹ Indeed, whereas stimulation of the cardiac β_1 AR is sufficient to promote cardiac contractility in mice without β_2 AR alone or without both β_1 AR and β_2 AR, these mice display altered metabolism in hearts.^{32,33} It remains to be examined whether the cardiac β_2 AR is necessary for contraction alone (eg, via stimulation of adenylyl cyclase with forskolin) to mediate increase in glucose uptake in the hearts. Nevertheless, these data support an essential role of the β_2 AR-Akt pathway in promoting glucose use in the heart.

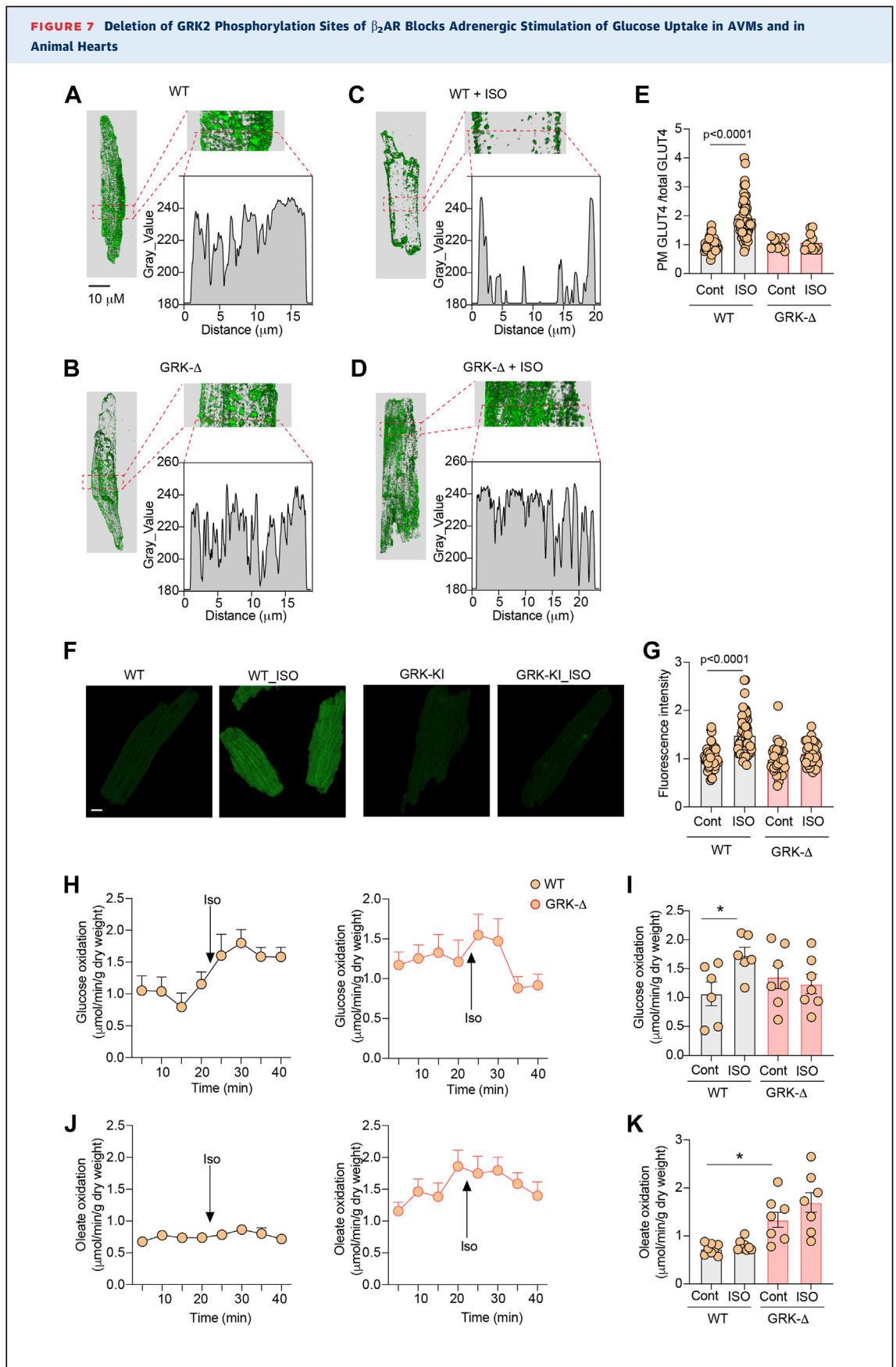
An important molecular mediator of intracellular GLUT4 tethering is the Rab guanosine triphosphatase-activating protein TBC1D4 (aka AS160).³⁴ AS160 displays guanosine triphosphatase-activating protein activity toward several Rab proteins, including Rab10 and Rab14, on purified GLUT4 vesicles²² and inhibits the translocation of the GLUT4 from intracellular

vesicles to the plasma membrane. Phosphorylation of AS160 at several Ser and Thr residues inhibits its guanosine triphosphatase-activating protein activity, thereby allowing GLUT4 translocation.³⁵ Two major kinases that are known to phosphorylate AS160 are AMPK and Akt.³⁰ AMPK functions as an “energy gauge” and is activated in response to increased AMP-ATP ratio.³⁶ Alternatively, AMPK can be activated in response to increased intracellular calcium levels via phosphorylation by the calcium-calmodulin-dependent kinases CAMKK1 and CAMKK2.^{37,38} Akt is typically triggered by PI3K activation. In the classical paradigm, stimulation of receptor tyrosine kinases (eg, insulin receptor) activates PI3K, leading to phosphatidylinositol (3,4,5)-trisphosphate production and phosphoinositide-dependent protein kinase 1 (PDK1) recruitment to the plasma membrane that can then phosphorylate and activate Akt.³⁹ However, insulin signaling is not required for sustaining cardiomyocyte metabolism, although it influences glucose uptake and mitochondrial oxidative capacity.^{10,40} Our data highlight that under adrenergic stimulation, the PI3K-Akt pathway is responsible for phosphorylation of AS160 and translocation of the GLUT4 for glucose uptake and metabolism in the heart. Whether the cardiac β_2 AR is required for the insulin-induced glucose uptake remains to be examined. Meanwhile, increased glucose is essential for cardiac protection during ischemia. Whereas the AMPK pathway is implicated in glucose metabolism during cardiac ischemia,^{41,42} activation of the cardiac β_2 AR also protects the myocardium from the ischemia-induced damage.^{43,44} It remains to be examined how the cardiac β_2 AR-dependent glucose metabolism could be linked to AMPK-mediated cardiac protection in ischemia.

GRKs can phosphorylate cardiac β_2 AR after agonist stimulation to regulate receptor signaling and function.⁴⁵ Among GRKs, GRK2 is among the major GRK isoforms expressed in the heart and phosphorylates the cardiac β_2 AR in myocytes.²⁶ Our data show that GRK2 and phosphorylation of β_2 AR at serine 355/356 are necessary for cardiac glucose uptake and metabolism. This reinforces the critical role of GRK2 in

FIGURE 6 Continued

(A to D) Representative confocal images of GLUT4 staining and **(F)** representative confocal images of 2-NBDG uptake in rat AVMs following stimulation with ISO (100 nmol/L, 30 minutes) or after pretreatment with GRK2 inhibitor paroxetine (PARO) (50 μ mol/L, 5 minutes) or fluoxetine (FLUO) (10 μ mol/L, 30 minutes) followed by stimulation with ISO. **(E, G)** Data represent mean \pm SEM of myocytes from 3 mice; $P < 0.0001$ were analyzed using 1-way analysis of variance with Tukey's multiple comparison test. **(H to K)** Representative confocal images of GLUT4 staining and **(M)** representative confocal images of 2-NBDG uptake in AVMs isolated from β_2 AR-CKO mice and expressing WT or mutant β_2 AR lacking the GRK phosphorylation sites at Ser355/356 (GRKmut- β_2 AR) after infection with recombinant adenovirus and after stimulation with ISO (100 nmol/L, 30 minutes). **(L, N)** Data represent mean \pm SEM of myocytes from 5 mice; $P < 0.0001$ were analyzed using Student's *t*-test. Abbreviations as in [Figures 1 to 3](#).



glucose metabolism reported previously,^{28,29} drawing comparison to another cardiac GRK, GRK5, which has been recently shown to phosphorylate the β_1 AR in the myocardium.⁴⁶ Increased expression of GRK2 has been observed in heart failure,⁴⁷ which may contribute to impaired glucose metabolism in the myocardium in part via phosphorylation and desensitization of the β_2 AR. Additionally, GRK2 phosphorylation of the β_2 AR at serine 355/356 is required for arrestin binding and receptor endocytosis.⁴⁸ It remains to be examined whether arrestin signaling and the subsequent receptor endocytosis are involved in GLUT4 translocation and glucose metabolism in the heart.

Conversion of glucose to glucose 6-phosphate by hexokinase is the first step in most glucose metabolic pathways. Subsequently, glucose 6-phosphate can be further metabolized through glycolysis, the pentose phosphate pathway, and the hexosamine biosynthetic pathway.^{3,49} The major route for glucose processing is glycolysis, which produces nicotinamide adenine dinucleotide and pyruvate. Pyruvate is further oxidized in the tricarboxylic acid cycle to generate reducing equivalents used for ATP synthesis. Our data show that the cardiac β_2 AR-Akt signaling increases glucose oxidation in the working hearts, potentially by increasing pyruvate oxidation in mitochondria. Although glycolysis is not the main source of ATP in a normal heart, it can be particularly important in pathological conditions or during ischemia.⁶ The pentose phosphate pathway is a critical source of cytosolic nicotinamide adenine dinucleotide phosphate that maintains reduced glutathione levels and regulates redox balance.⁵⁰ Finally, the hexosamine biosynthetic pathway generates uridine diphosphate N-acetylglucosamine, which is used for O-GlcNAcylation, a prominent post-translational modification of O-linked b-N-acetylglucosamine (O-GlcNAc).⁵¹ O-GlcNAcylation plays a critical role in sensing nutrient levels, cell stressors, and cell cycle alteration.⁵¹ The potential role of the cardiac β_2 AR-Akt signaling in glucose

metabolism in the pentose phosphate and hexosamine biosynthetic pathways remains to be examined.

In summary, our data define a cardiac β_2 AR-Akt pathway essential for cardiac glucose metabolism under adrenergic stimulation. However, the study does not address the impact of calcium and contractility on glucose uptake in isolated myocytes, which can be done with AVMs under pacing condition. The current study does not examine adrenergic regulation of glucose uptake in vivo, which can be compared to the data from the current ex vivo study on working hearts. Given the connection between insulin signaling and cardiac adrenergic receptor reported previously,^{52,53} a possible role of β_2 AR in insulin-induced glucose uptake remains to be determined. The experiments are limited to male mice. Future studies remain to examine the potential sex-specific effects on adrenergic regulation of glucose uptake between male and female mice.^{54,55} The role of β_2 AR in regulation of glucose uptake and metabolism in cardiac diseases remains to be explored.

FUNDING SUPPORT AND AUTHOR DISCLOSURES

Dr Zhu has received an American Heart Association postdoctoral fellowship. Dr Li has received support from National Institutes of Health grants (R01HL158515, R01GM124108) and U.S. Department of Veterans Affairs' VA Merit Award (101BX005625). Dr Xiang has received support from National Institutes of Health grants (R01-HL147263, R01-HL162825) and U.S. Department of Veterans Affairs' VA Merit Awards (01BX002900, 01BX005100); and is an established investigator of the American Heart Association. All other authors have reported that they have no relationships relevant to the contents of this paper to disclose.

ADDRESS FOR CORRESPONDENCE: Dr Yang K. Xiang, Department of Pharmacology, University of California at Davis, 1 Shields Avenue, Davis, California 95655, USA. E-mail: ykxiang@ucdavis.edu. Twitter: [@kevinxyxiang](https://twitter.com/kevinxyxiang). OR Dr Ji Li, Professor of Physiology, Department of Surgery, Pharmacology, and Medical Engineering, 12901 Bruce B. Downs Boulevard, MDC 110 (Office: MDC 4106B), Tampa, Florida 33612, USA. E-mail: jili@usf.edu.

FIGURE 7 Continued

(A to D) Representative confocal images of GLUT4 staining and (F) representative confocal images of 2-NBDG uptake in AVMs isolated from WT or GRKD mice and after stimulation with ISO (100 nmol/L, 30 minutes). (E, G) Data represent mean \pm SEM of myocytes from 3 mice; $P < 0.0001$ were analyzed using two-way analysis of variance with Tukey's multiple comparison test. (H to K) Time course and peak response in glucose oxidation (H,I) and oleate oxidation (J, K) before and after stimulation with ISO (100 nmol/L) in WT and GRKD mice. Data represent mean \pm SEM, $n = 8$; $*P < 0.05$ were obtained using two-way analysis of variance with Tukey's multiple comparison test.

PERSPECTIVES

COMPETENCY IN MEDICAL KNOWLEDGE: Myocardial glucose oxidation is reduced in heart failure and with diabetes and obesity, where fatty acid oxidation is increased. Glucose metabolism is essential for protect the heart against ischemic damage. Our studies have identified cardiac β_2 AR as an important regulator of cardiac metabolism that could be modulated in a broad range of heart diseases.

TRANSLATIONAL OUTLOOK: This work presents evidence that cardiac glucose metabolism can be modulated by cardiac β_2 AR in heart diseases. The GRK2-mediated cardiac β_2 AR-Akt pathway presents a potential therapeutic target to restore cardiac glucose metabolism in ischemic and failing hearts.

REFERENCES

- Neubauer S. The failing heart—an engine out of fuel. *N Engl J Med*. 2007;356(11):1140-1151.
- Stanley WC, Recchia FA, Lopaschuk GD. Myocardial substrate metabolism in the normal and failing heart. *Physiol Rev*. 2005;85(3):1093-1129.
- Tran DH, Wang ZV. Glucose metabolism in cardiac hypertrophy and heart failure. *J Am Heart Assoc*. 2019;8(12):e012673.
- Bertrand L, Auquier J, Renguier E, et al. Glucose transporters in cardiovascular system in health and disease. *Pflugers Arch*. 2020;472(9):1385-1399.
- Shao D, Tian R. Glucose transporters in cardiac metabolism and hypertrophy. *Compr Physiol*. 2015;6(1):331-351.
- Chanda D, Luiken JJ, Glatz JF. Signaling pathways involved in cardiac energy metabolism. *FEBS Lett*. 2016;590(15):2364-2374.
- Nishimura H, Pallardo FV, Seidner GA, Vannucci S, Simpson A, Birnbaum MJ. Kinetics of GLUT1 and GLUT4 glucose transporters expressed in Xenopus oocytes. *J Biol Chem*. 1993;268(12):8514-8520.
- Wheeler TJ, Fell RD, Hauck MA. Translocation of two glucose transporters in heart: effects of rotenone, uncouplers, workload, palmitate, insulin and anoxia. *Biochim Biophys Acta*. 1994;1196(2):191-200.
- Egert S, Nguyen N, Schwaiger M. Contribution of alpha-adrenergic and beta-adrenergic stimulation to ischemia-induced glucose transporter (GLUT) 4 and GLUT1 translocation in the isolated perfused rat heart. *Circ Res*. 1999;84(12):1407-1415.
- Abel ED. Insulin signaling in the heart. *Am J Physiol Endocrinol Metab*. 2021;321(1):E130-E145.
- Thorp AA, Schlaich MP. Relevance of sympathetic nervous system activation in obesity and metabolic syndrome. *J Diabetes Res*. 2015;2015:341583.
- Nevezorova J, Evans BA, Bengtsson T, Summers RJ. Multiple signalling pathways involved in beta2-adrenoceptor-mediated glucose uptake in rat skeletal muscle cells. *Br J Pharmacol*. 2006;147(4):446-454.
- Ngala RA, O'Dowd J, Wang SJ, et al. Metabolic responses to BRL37344 and clenbuterol in soleus muscle and C2C12 cells via different atypical pharmacologies and beta2-adrenoceptor mechanisms. *Br J Pharmacol*. 2008;155(3):395-406.
- Ishiyama-Shigemoto S, Yamada K, Yuan X, Ichikawa F, Nonaka K. Association of polymorphisms in the beta2-adrenergic receptor gene with obesity, hypertriglyceridaemia, and diabetes mellitus. *Diabetologia*. 1999;42(1):98-101.
- Cipolletta E, Del Giudice C, Santulli G, Trimarco B, Iaccarino G. Opposite effects of beta2-adrenoceptor gene deletion on insulin signaling in liver and skeletal muscle. *Nutr Metab Cardiovasc Dis*. 2017;27(7):615-623.
- Gjesing AP, Andersen G, Burgdorf KS, et al. Studies of the associations between functional beta2-adrenergic receptor variants and obesity, hypertension and type 2 diabetes in 7,808 white subjects. *Diabetologia*. 2007;50(3):563-568.
- Madamanchi A. Beta-adrenergic receptor signaling in cardiac function and heart failure. *McGill J Med*. 2007;10(2):99-104.
- Zhang W, Yano N, Deng M, Mao Q, Shaw SK, Tseng Y-T. β -adrenergic receptor-PI3K signaling crosstalk in mouse heart: elucidation of immediate downstream signaling cascades. *PLoS One*. 2011;6(10):e26581.
- Cipolletta E, Campanile A, Santulli G, et al. The G protein coupled receptor kinase 2 plays an essential role in beta-adrenergic receptor-induced insulin resistance. *Cardiovasc Res*. 2009;84(3):407-415.
- DeWire SM, Ahn S, Lefkowitz RJ, Shenoy SK. Beta-arrestins and cell signaling. *Annu Rev Physiol*. 2007;69:483-510.
- Usui I, Imamura T, Satoh H, et al. GRK2 is an endogenous protein inhibitor of the insulin signaling pathway for glucose transport stimulation. *EMBO J*. 2004;23(14):2821-2829.
- Anis Y, Leshem O, Reuveni H, et al. Antidiabetic effect of novel modulating peptides of G-protein-coupled kinase in experimental models of diabetes. *Diabetologia*. 2004;47(7):1232-1244.
- Tseng CC, Zhang XY. Role of G protein-coupled receptor kinases in glucose-dependent insulinotropic polypeptide receptor signaling. *Endocrinology*. 2000;141(3):947-952.
- Reddy GR, West TM, Jian Z, et al. Illuminating cell signaling with genetically encoded FRET biosensors in adult mouse cardiomyocytes. *J Gen Physiol*. 2018;150(11):1567-1582.
- West TM, Wang Q, Deng B, et al. Phosphodiesterase 5 associates with beta2 adrenergic receptor to modulate cardiac function in type 2 diabetic hearts. *J Am Heart Assoc*. 2019;8(15):e012273.
- Liu R, Ramani B, Soto D, De Arcangelis V, Xiang Y. Agonist dose-dependent phosphorylation by protein kinase A and G protein-coupled receptor kinase regulates beta2 adrenoceptor coupling to G(i) proteins in cardiomyocytes. *J Biol Chem*. 2009;284(47):32279-32287.
- Wang L, Quan N, Sun W, et al. Cardiomyocyte-specific deletion of Sirt1 gene sensitizes myocardium to ischaemia and reperfusion injury. *Cardiovasc Res*. 2018;114(6):805-821.
- Sato PY, Chuprun JK, Grisanti LA, et al. Restricting mitochondrial GRK2 post-ischemia confers cardioprotection by reducing myocyte death and maintaining glucose oxidation. *Sci Signal*. 2018;11(560):ea0144.
- Cicarelli M, Chuprun JK, Rengo G, et al. G protein-coupled receptor kinase 2 activity impairs cardiac glucose uptake and promotes insulin resistance after myocardial ischemia. *Circulation*. 2011;123(18):1953-1962.
- Montessuit C, Lerch R. Regulation and dysregulation of glucose transport in cardiomyocytes. *Biochim Biophys Acta*. 2013;1833(4):848-856.
- Luiken JJ, Glatz JF, Neumann D. Cardiac contraction-induced GLUT4 translocation requires dual signaling input. *Trends Endocrinol Metab*. 2015;26(8):404-410.
- Chruscinski AJ, Rohrer DK, Schauble E, Desai KH, Bernstein D, Kobilka BK. Targeted disruption of the beta2 adrenergic receptor gene. *J Biol Chem*. 1999;274(24):16694-16700.
- Rohrer DK, Chruscinski A, Schauble EH, Bernstein D, Kobilka BK. Cardiovascular and

- metabolic alterations in mice lacking both beta1- and beta2-adrenergic receptors. *J Biol Chem.* 1999;274(24):16701-16708.
34. Satoh T. Molecular mechanisms for the regulation of insulin-stimulated glucose uptake by small guanosine triphosphatases in skeletal muscle and adipocytes. *Int J Mol Sci.* 2014;15(10):18677-18692.
35. Stockli J, Davey JR, Hohnen-Behrens C, Xu A, James DE, Ramm G. Regulation of glucose transporter 4 translocation by the Rab guanine nucleotide exchange factor 1 protein AS160/TBC1D4: role of phosphorylation and membrane association. *Mol Endocrinol.* 2008;22(12):2703-2715.
36. Russell RR 3rd, Bergeron R, Shulman GI, Young LH. Translocation of myocardial GLUT-4 and increased glucose uptake through activation of AMPK by AICAR. *Am J Physiol.* 1999;277(2):H643-H649.
37. Hawley SA, Pan DA, Mustard KJ, et al. Calmodulin-dependent protein kinase kinase-beta is an alternative upstream kinase for AMP-activated protein kinase. *Cell Metab.* 2005;2(1):9-19.
38. Woods A, Dickerson K, Heath R, et al. Ca²⁺/calmodulin-dependent protein kinase kinase-beta acts upstream of AMP-activated protein kinase in mammalian cells. *Cell Metab.* 2005;2(1):21-33.
39. Bertrand L, Horman S, Beauloye C, Vanoverschelde J-L. Insulin signalling in the heart. *Cardiovasc Res.* 2008;79(2):238-248.
40. Zhu Y, Pereira RO, O'Neill BT, et al. Cardiac PI3K-Akt impairs insulin-stimulated glucose uptake independent of mTORC1 and GLUT4 translocation. *Mol Endocrinol.* 2013;27(1):172-184.
41. Cao Y, Bojjireddy N, Kim M, et al. Activation of gamma2-AMPK suppresses ribosome biogenesis and protects against myocardial ischemia/reperfusion injury. *Circ Res.* 2017;121(10):1182-1191.
42. Young LH, Li J, Baron SJ, Russell BR. AMP-activated protein kinase: a key stress signaling pathway in the heart. *Trends Cardiovasc Med.* 2005;15(3):110-118.
43. Wang DW, Liu M, Wang P, Zhan X, Liu Y-Q, Zhao L-S. ADRB2 polymorphisms predict the risk of myocardial infarction and coronary artery disease. *Genet Mol Biol.* 2015;38(4):433-443.
44. Rorth R, Fosbol EL, Mogensen UM, et al. The importance of beta2-agonists in myocardial infarction: Findings from the Eastern Danish Heart Registry. *Eur Heart J Acute Cardiovasc Care.* 2016;5(8):551-559.
45. Nobles KN, Xiao K, Ahn S, et al. Distinct phosphorylation sites on the beta(2)-adrenergic receptor establish a barcode that encodes differential functions of beta-arrestin. *Sci Signal.* 2011;4(185):ra51.
46. Xu B, Li M, Wang Y, et al. GRK5 controls SAP97-dependent cardiotoxic beta1 adrenergic receptor-CaMKII signaling in heart failure. *Circ Res.* 2020;127(6):796-810.
47. Iaccarino G, Barbato E, Cipolletta E, et al. Elevated myocardial and lymphocyte GRK2 expression and activity in human heart failure. *Eur Heart J.* 2005;26(17):1752-1758.
48. Vaughan DJ, Millman EE, Godines V, et al. Role of the G protein-coupled receptor kinase site serine cluster in beta2-adrenergic receptor internalization, desensitization, and beta-arrestin translocation. *J Biol Chem.* 2006;281(11):7684-7692.
49. Doenst T, Nguyen TD, Abel ED. Cardiac metabolism in heart failure: implications beyond ATP production. *Circ Res.* 2013;113(6):709-724.
50. Stincone A, Prigione A, Cramer T, et al. The return of metabolism: biochemistry and physiology of the pentose phosphate pathway. *Biol Rev Camb Philos Soc.* 2015;90(3):927-963.
51. Bolanle IO, Palmer TM. Targeting protein O-GlcNAcylation, a link between type 2 diabetes mellitus and inflammatory disease. *Cells.* 2022;11(4):705.
52. Wang Q, Liu Y, Fu Q, et al. Inhibiting insulin-mediated beta2-adrenergic receptor activation prevents diabetes-associated cardiac dysfunction. *Circulation.* 2017;135(1):73-88.
53. Fu Q, Xu B, Liu Y, et al. Insulin inhibits cardiac contractility by inducing a Gi-biased beta2-adrenergic signaling in hearts. *Diabetes.* 2014;63(8):2676-2689.
54. Kakinuma Y, Okada S, Nogami M, Kumon Y. The human female heart incorporates glucose more efficiently than the male heart. *Int J Cardiol.* 2013;168(3):2518-2521.
55. Peterson LR, Herrero P, Coggan AR, et al. Type 2 diabetes, obesity, and sex difference affect the fate of glucose in the human heart. *Am J Physiol Heart Circ Physiol.* 2015;308(12):H1510-H1516.

KEY WORDS adrenergic receptor, Akt substrate of 160 kDa, glucose oxidation, glucose transporter 4, glucose uptake, G-protein receptor kinase 2

APPENDIX For supplemental figures, tables, and data sets, please see the online version of this paper.